Static Stability and Control Characteristics of Scissor Wing Configurations

Kamran Rokhsaz* and Bruce P. Selberg†
University of Missouri, Rolla, Rolla, Missouri 65401

A scissor wing geometry is introduced as an alternative to variable sweep and oblique wing designs. It is shown that this configuration offers certain enhancements to the stability and control of the aircraft in addition to aerodynamic advantages associated with sweep. It is shown that a scissor wing configuration can maintain a constant static margin throughout its flight Mach numbers. The dependence of the motion of the aircraft neutral point on the sweep angle is shown to be a function of the chord and span ratios. The control authority is studied and shown not to suffer with changes in the sweep angle. It is also suggested that with the use of wing mounted elevons, additional pitch and attitude control can be obtained over a range of sweep angles.

Nomenclature

b = wing span
$\bar{C}$ = average chord
C_L = lift coefficient
C_{L_α} = $\partial C_L/\partial\alpha$
$C_{L_{\delta_e}}$ = $\partial C_L/\partial\delta_e$
C_l = rolling-moment coefficient
$C_{l_{\delta_a}}$ = $\partial C_l/\partial\delta_a$
C_m = pitching-moment coefficient
C_{m_α} = $\partial C_m/\partial\alpha$
$C_{m_{\delta_e}}$ = $\partial C_m/\partial\delta_e$
M = Mach number
p = roll rate
q = pitch rate
Æ = aspect ratio
S = reference area
α = angle of attack
δ_a = aileron deflection
δ_e = elevator deflection
Λ = sweep angle

Subscripts

b = base line
cp = center of pressure
f = front wing
r = rear wing

Introduction

AERODYNAMIC requirements for low-speed, high-lift flight with maneuverability and high-speed flight are inherently conflicting. On the one hand, at low speeds, it is desirable to have high aspect ratios to reduce the induced drag and to increase the overall lift-curve slope of the aircraft. On the other hand, at high speeds, the very same characteristics of a high aspect ratio wing manifest themselves as liabilities in terms of wave drag and gust loading. Furthermore, in supersonic flight, the center of pressure of the aircraft usually shifts back, leading to relatively large changes in the static margin. These changes generally result in relatively large trim drags and partial loss of maneuverability.

One of the attempts at bringing together both sets of requirements is the use of variable geometry. Variable sweep wings in which both halves of the wing can be swept back for high-speed flight have been employed in several aircraft. However, this can result in additional backward shifts of the center of pressure. One possible solution is to use fuel transfer in order to move the aircraft center of gravity as well. However, such a solution appears impractical for a fighter/attack aircraft of high weight density. Another solution is to have the wings pivoted about a point far outboard of the fuselage center line and become partially covered in the swept mode, as suggested by Alford and Polhamus.[1] Both of these factors result in mechanical complexities and added structural weight. These are the results of having to strengthen the inboard part of the wing to accommodate the actuation mechanism and to withstand the torsional moment produced by the swept outboard part. Furthermore, the actuation mechanism also requires extra parts to insure synchronized sweeping of both sides.

A possible alternative has been suggested by R. T. Jones in Ref. 2, among numerous other articles. In this concept, the entire wing is to be rotated about midspan. While this appears to be a viable solution to the problem, the concept inherently produces nonsymmetric aerodynamic forces and moments, leading to handling problems as shown by Fantino et al.[3] Among these problems are the nonsymmetric pitching moment induced by the ailerons and the side forces generated by the wing producing a sideslip. This sideslip has to be countered by either tilting the wing or banking the entire aircraft. The former solution requires rather complex hinges, whereas the latter is totally unacceptable from the view point of handling qualities.

The concept of the scissor wing, introduced in Ref. 4, seems to take advantage of the positive points of both of the aforementioned ideas, plus some. In this design, it is proposed to use two wings sweeping in the opposite directions. This allows both wings to be swept about a pivot point on the center line of the fuselage. The actuation mechanism is located in the

Presented as Paper 89-0013 at the 27th Aerospace Sciences Meeting, Reno, NV, Jan. 9–12, 1989; received Feb. 2, 1989; revision received Oct. 30, 1989.

*Lecturer, Mechanical and Aerospace Engineering and Engineering Mechanics. Senior Member AIAA.

†Professor, Mechanical and Aerospace Engineering and Engineering Mechanics. Associate Fellow AIAA.

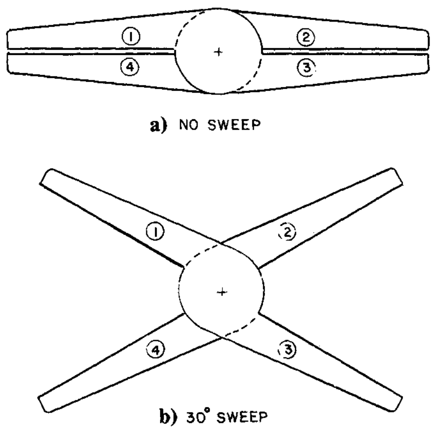

Fig. 1 Representative geometry.

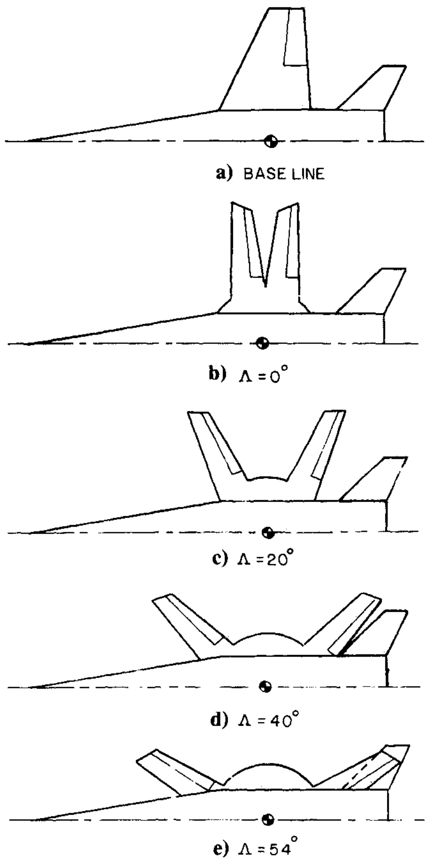

Fig. 2 Baseline and equivalent scissor wing (control surfaces not to scale).

fuselage, and the synchronization of the sweep is not as critical as that in the case of a variable sweep geometry. With this system, at low speeds, the sweep angle is minimized for maximum efficiency and maneuverability. On the other hand, at high speeds, when gust loading and wave drag become strong, the wings can be swept to alleviate both problems. Furthermore, this arrangement has none of the handling problems of the oblique wing due to its total symmetry. Additionally, this unique configuration allows the designer to manipulate the static margin and longitudinal control of the aircraft through wing sweep.

It is the objective of this paper to explore the effects of the sweep angle on the static stability and control of the scissor wing configurations. It is intended to show the effect of the sweep angle on the aircraft static margin and demonstrate certain enhancements in the longitudinal control of the aircraft. None of the configurations presented here have been optimized in any respect.

Method of Analysis

The vortex lattice method of Tulinius[5] was used to obtain the aerodynamic characteristics of the configurations under study. A detailed description of this method can be found in Refs. 6 and 7. In this method, lifting surfaces are replaced by their mean camber lines and divided into small panels. Each panel is assigned a horseshoe vortex with the bound vortex on the quarter length of the panel and a control point on the three quarter length where flow tangency condition is satisfied. Subsonic compressibility effects are accounted for by using the Prandtl-Glauert transformation. Supersonic vortices are used for supersonic flow. Therefore, the method is limited to the linear range of aerodynamics, which precludes any transonic calculations. Also, the computer program based on this method was limited to 200 panels, which in some cases resulted in slight numerical oscillations. Although the absolute results predicted by one numerical technique may not be quantitatively accurate, the predicted trends are valid. Also, firm conclusions can be made if the same method is used for comparison of two geometries.

Before applying this method to an aircraft, the characteristics of three sets of scissor wings with no fuselage or tail were studied. This allowed establishing certain trends about the motion of the center of pressure of the wing. Figure 1 shows one of these geometries in the swept case as well as in the unswept mode.

Later, for the purpose of a more objective comparison, the conventional configuration shown in Fig. 2a was employed as the base line. The center of gravity in this case was placed at a point resulting in 15% static instability at zero Mach number. This value was deemed as reasonable for a statically unstable configuration. Although all calculations were made for this location of the center of gravity, the same effects were present at other values of static margin as well. The stabilizer was assumed to act as an elevon in addition to 12% chord ratio ailerons on the wing. Figures 2b through 2e also show the

Table 1 Model characteristics

Parameter	Base line	Scissor wing
S^a	0.4689	0.4689
b	1.0000	1.0847
AR	2.1326	2.5129
$\bar{c}$	0.4689	0.4323
λ	0.3265	0.4500 (each)
C_{m_α}	0.3673 rad^{-1}	0.3761 rad^{-1}
C_{L_α}	2.3690 rad^{-1}	2.4211 rad^{-1}
$C_{L_{\delta_e}}$	0.3754 rad^{-1}	0.2253 rad^{-1}
$C_{m_{\delta_e}}$	−0.2131 rad^{-1}	−0.1822 rad^{-1}
$C_{l_{\delta_a}}{}^b$	−0.0470 rad^{-1}	−0.0367 rad^{-1}
$C_{l_{\delta_a}}{}^c$	−0.0667 rad^{-1}	−0.0955 rad^{-1}
$\partial C_m/\partial q$	−0.8649 s/rad	−0.6772 s/rad
$\partial C_l/\partial p$	−0.1889 s/rad	−0.2070 s/rad

[a]All lengths are nondimensional with respect to the base-line wing span.
[b]Due to the tail only.
[c]Due to the wing only (both wings for the scissor wing).

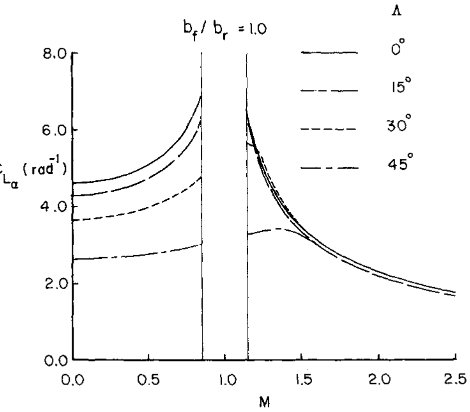

Fig. 3 Lift curve slope of the representative geometry.

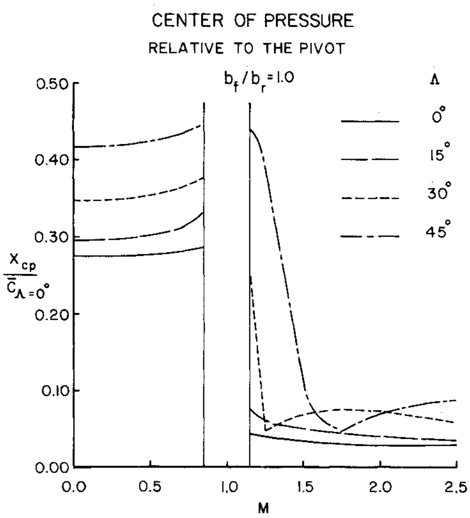

Fig. 4 Center of pressure of the representative geometry.

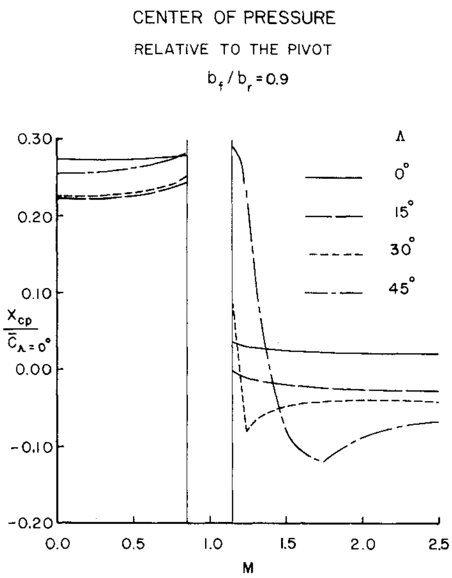

Fig. 5 Center of pressure for unequal spans.

equivalent scissor wing design under consideration, for different sweep angles. The reader should be cautioned that the control surfaces in this figure have not been drawn to scale. For the base line, no vertical gap between the wing and tail was used. However, to avoid geometric interference, the tail was placed at 8.5% span below the wing for the scissor wing geometries. All airfoils were assumed to be thin and symmetric. The same total lifting area and static margin were used for the base line and the unswept scissor wing. This provided configuration comparisons of nearly equal wing loading, same total wetted area, and trim drag. Each wing was assumed to be fitted with elevons in addition to the tail. Also, it was assumed that the center of gravity of the scissor wing remained invariant with sweep angle. This appeared to be a reasonable assumption because the pivot was assumed to be at the mid chord of the wing root and the wings had equal spans. In the swept cases, even though the exposed area, the wing span, and the effective chord were different, those of the unswept configuration were used as reference quantities. The effectiveness of every control surface was calculated at zero angle of attack by dividing the respective forces and moments by the small corresponding control-surface deflection. Table 1 shows these values for the base line geometry at zero Mach number as well as for the scissor wing with zero sweep. For clarity, sweep angle here refers to the sweep of the leading edge of the front wing.

Results and Discussion

Figure 3 shows the lift-curve slope of the geometry shown in Fig. 1. As expected, lift-curve slope decreases with increasing sweep angle. This is not only due to increased sweep but also due to reduced effective aspect ratio. In this figure, Mach numbers of 0.85–1.15 were omitted because they were clearly in the transonic range and out of the domain of validity of the computer program. It may be argued that even a Mach number of 0.85 is rather presumptuous in conjunction with linear theory, but transonic effects should not be very strong at this Mach number for supercritical airfoils. Figure 4 shows the center of pressure for the same geometry at different values of the sweep angle and Mach number. It is clearly evident from this figure that the center of pressure of the wing shifts forward with increasing sweep angle. This is the direct consequence of the aerodynamic coupling between the wings. In the presence of such coupling, the lift curve slope of the front wing is much larger than that of an uncoupled wing, whereas the lift curve slope of the rear wing is much smaller than that of a single wing. Therefore, increasing the sweep angle causes the overall center of pressure to move slightly forward. As the sweep angle increases, this coupling tends to diminish. Because this point and the aerodynamic center of the wing are closely associated, this behavior would indicate a decrease in the static margin of an aircraft if it were to be equipped with this wing.

In order to demonstrate that these shifts of the center of pressure can be manipulated to an optimum degree by the aircraft designer, this parameter was calculated for two other geometries as well. Figure 5 represents the results for a wing similar to that of Fig. 1, except with the front wing span 10% shorter than the rear wing span. As seen in this figure, sweep angle changes the location of the center of pressure only slightly in the subsonic case. However, in the supersonic flow, this point moves aft with increasing sweep, aggravating the compressibility effects. On the other hand, if the spans are maintained equal with the front wing having twice the chord length of the rear wing, variation of the sweep angle would

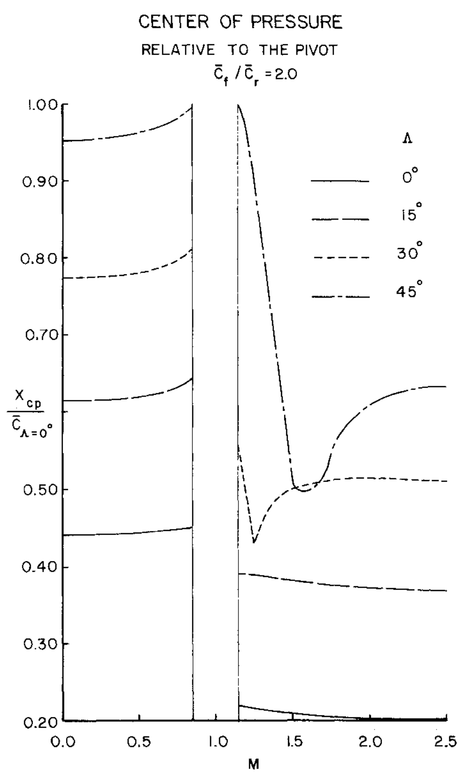

Fig. 6 Center of pressure for unequal chords.

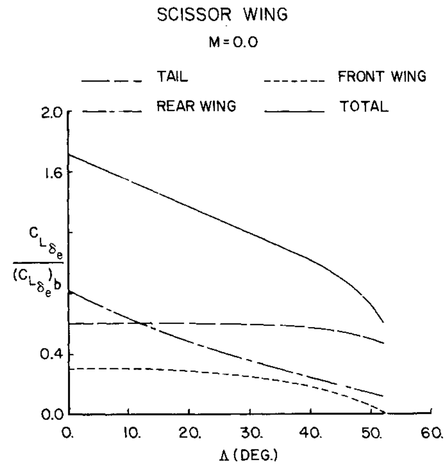

Fig. 7 Effect of sweep on $C_{L_{\delta_e}}$.

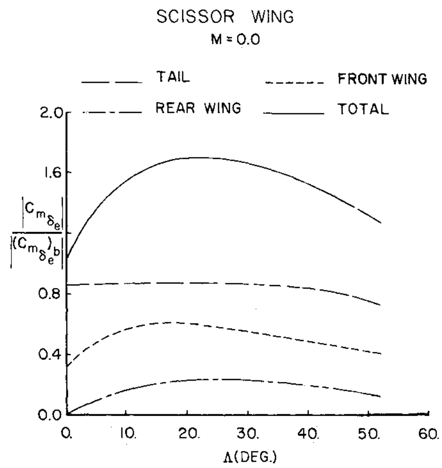

Fig. 8 Effect of sweep on pitch-control derivative.

cause large changes in the center of pressure. This case is depicted in Fig. 6. However, in this case, there is very little difference in the location of this point between a sweep of 15 deg in subsonic flow and 45 deg in supersonic flow. Therefore, it remains to the designer to choose the proper chord and span ratios in order to accommodate the specific design requirements.

Geometries represented in Fig. 2 were used to study the effectiveness of different control surfaces. All these derivatives were calculated at zero Mach number for varying sweep angles. However, the effects of Mach number on the longitudinal static stability of the aircraft was also considered. All moments were taken about a fixed assumed center of gravity location resulting in -15% static margin at zero Mach number for the base line and zero sweep for the scissor wing. These results are presented in the following subsections.

Longitudinal Control

Figures 7 and 8 show the effects of the elevator deflection on the total aircraft lift and pitching-moment coefficients. Because the horizontal tail locations are not the same, these derivatives are slightly different for the scissor wing and the base line. As expected, the effectiveness of the wing mounted elevons somewhat diminishes with increasing sweep angle. However, this does not necessarily translate into loss of elevator authority. As the sweep angle increases, the effective lifting area of the aircraft decreases. Furthermore, as is evident in Fig. 8, the front wing elevons now begin to offer a strong influence on the aircraft pitching moment. This is quite natural because at moderate sweep angles, the scissor wing configuration becomes very similar to a three-surface geometry. In fact under these conditions, the combination of the tail and front wing can be used to trim the aircraft at arbitrary attitudes for a fixed air speed.

Figure 9 shows the pitch damping derivative as a function of the sweep angle at zero Mach number. As would be expected, this derivative sharply rises with increasing sweep. However, this should not result in any significant loss of control authority. To demonstrate this point, one can consider the following approximation. About the pitch axis

$$(i_B D - C_{m_q})\hat{q} = C_{m_{\delta_e}}\delta_e \tag{1}$$

where $\hat{q}$, $\hat{t}$, and i_B represent the nondimensional pitch rate, time, and mass moment of inertia, respectively. In response to a unit step function deflection of the elevator,

$$\hat{q} = C_{m_{\delta_e}}\delta_e\left[\exp\left(\frac{C_{m_q}}{i_B}\hat{t}\right) - 1\right]/C_{m_q} \tag{2}$$

and

$$D\hat{q} = C_{m_{\delta_e}}\delta_e \exp\left(\frac{C_{m_q}}{i_B}\hat{t}\right)/i_B \tag{3}$$

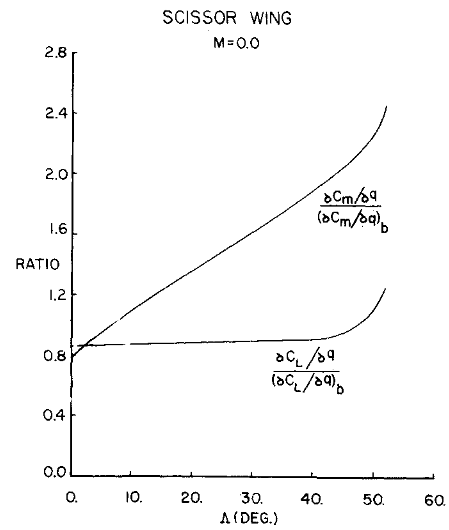

Fig. 9 Effect of sweep on pitch-damping derivative.

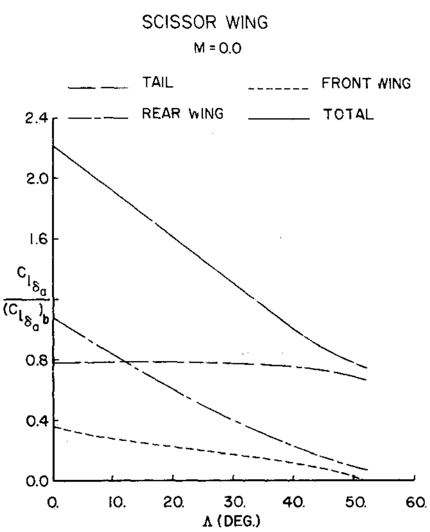

Fig. 10 Effect of sweep on roll-control derivative.

Now if control authority is defined as the initial angular acceleration of the aircraft due to the elevator input (i.e., $\hat{t} = 0$), then

$$\frac{D\hat{q}(\hat{t} = 0)}{\delta_e} = \frac{C_{m_{\delta_e}}}{i_B} \tag{4}$$

As the sweep angle increases, the mass moment of inertia about the pitch axis also increases. However, because $C_{m_{\delta_e}}$ is much larger than that of the base line, increasing i_B will not affect the pitch authority compared with the base line. On the other hand, if control authority is defined as the ultimate pitch rate (i.e., $\hat{t} \to \infty$), then

$$\frac{\hat{q}(\hat{t} \to \infty)}{\delta_e} = -\frac{C_{m_{\delta_e}}}{C_{m_q}} \tag{5}$$

In this case, as the sweep increases, C_{m_q} increases resulting in some loss of pitch rate. However, this loss will not be realized until sweep angle becomes larger than approximately 40 deg, as indicated from Figs. 8 and 9.

Lateral Control

Figure 10 shows the aileron effectiveness of the geometry under consideration. It is quite evident from this figure that the effectiveness of the wing mounted ailerons diminishes quite rapidly with sweep. But the tail appears to remain insensitive to the wing sweep, despite the strong aerodynamic coupling between the two. Again, much like the longitudinal case, the apparent reduction in the aileron effectiveness should not be any cause for alarm for the following reasons.

1) This derivative is a function of the wing area and the wing span. Both of these parameters decrease with increasing sweep. However, these effects are not reflected in Fig. 10 because the reference area and span were maintained constant throughout these calculations.

2) Roll damping derivative also decreases rapidly with sweep, as shown in Fig. 11.

3) The mass moment of inertia of the aircraft about the roll axis decreases with the square of the cosine of the sweep angle.

A simple model similar to that of the previous subsection will demonstrate that control authority actually increases with increasing sweep angle.

Longitudinal Stability

Lift and pitching moment curve slopes are depicted in Fig. 12. As shown here, lift curve slope decreases predictably with increased sweep angle. Reference was made to reduced gust loading at large sweep angles. This parameter is directly proportional to the aircraft lift curve slope. Therefore, any reduction in this derivative results in reduced gust loading with all other parameters being the same. The reader should be cautioned that although the magnitude of C_{m_α} increases with increasing sweep angle, this actually indicates a *reduction* in longitudinal stability. The reason for this rests in the fact that all configurations considered here were statically unstable. This can be seen more clearly in Fig. 13. Static margin in these figures was calculated from the ratio of ΔC_{m_α} and ΔC_{L_α}. This figure clearly indicates a reduction in longitudinal stability as a function of sweep angle, which is consistent with the results shown in Fig. 4. Also, this figure clearly shows that in the supersonic range, by varying the sweep angle, a preset static margin can be maintained at any Mach number.

The results presented here should be interpreted as being very preliminary. Many other aspects of scissor wing configurations need to be studied in detail. These include, but are not limited to, high angle of attack characteristics in conjunction with strakes, wing-rock tendencies at all sweep angles, and other aerodynamic payoffs in light of the added structural weight.

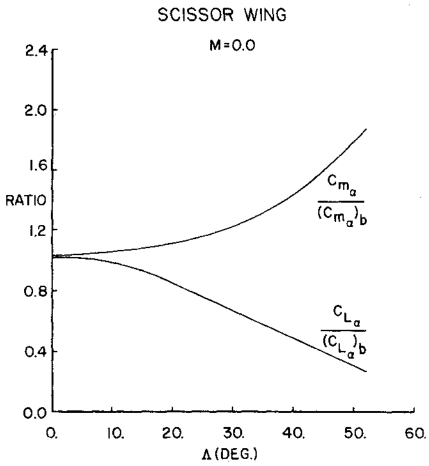

Fig. 12 Effect of sweep on C_{L_α} and C_{m_α}.

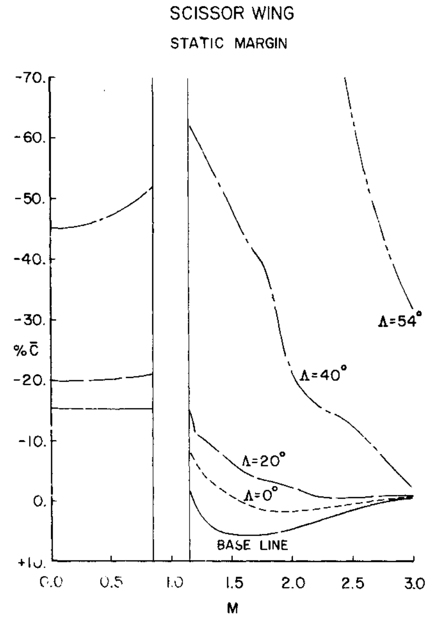

Fig. 13 Effect of Mach number and sweep on static margin.

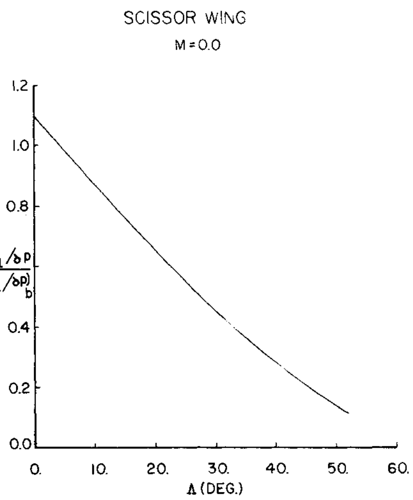

Fig. 11 Effect of sweep on roll-damping derivative.

Conclusions

A scissor wing geometry was introduced as an alternative to variable sweep and oblique wing designs. Comparisons were made with an equivalent fixed wing geometry.

1) It was demonstrated that this configuration, even in the nonoptimized form, can enhance the stability and control of the aircraft by maintaining a fixed, static margin throughout the range of flight Mach numbers.

2) It was shown that by proper selection of span and chord ratios, the dependence of the neutral point, and therefore the static margin, on the sweep angle can be manipulated.

3) The effectiveness of the control surfaces was studied at different sweep angles. No major loss of control effectiveness was detected and in fact in some cases, additional maneuverability was shown to be possible.

4) The use of wing-mounted elevons was suggested to allow trim at arbitrary incidence angles for a fixed air speed.

References

[1]Alford, W. J., and Polhamus, E. C., "Variable Sweep Wing Configuration," United States Patent No. 3053484, 1962.

[2]Jones, R. T., "Oblique-Wing Supersonic Aircraft," United States Patent No. 3971535, 1976.

[3]Fantino, R. E., Parsons, E. K., Powell, J. D., and Shevell, R. S., "Effects of Asymmetry on the Dynamic Stability of Aircraft," NASA CR-142857, 1975.

[4]Rokhsaz, K., "Scissor Wing-Patent Disclosure," Disclosure No. 87-UMR-023, 1986.

[5]Tulinius, J., "Unified Subsonic, Transonic, and Supersonic NAR Vortex Lattice," North American Rockwell, TFD-72-523, 1972.

[6]Moran, J., *An Introduction to Theoretical and Computational Aerodynamics*, Wiley, New York, 1984.

[7]Bertin, J. J., and Smith M. L., *Aerodynamics for Engineers*, Prentice-Hall, Englewood Cliffs, NJ, 1979.